Journal of Applied Polymer Science

# Electrical Conductivity and Tensile Properties of Block-Copolymer-Wrapped Single-Walled Carbon Nanotube/Poly(methyl methacrylate) Composites

**Alejandro Ansón-Casaos,[1] F. Javier Pascual,[2,3] Cristina Ruano,[4] Natalia Fernández-Huerta,[1] Isaías Fernández-Pato,[1] Juan C. Otero,[4] J. Antonio Puértolas,[3] M. Teresa Martínez[1]**

[1]Instituto de Carboquímica, ICB-CSIC, Zaragoza 50018, Spain

[2]Centro Universitario de la Defensa de Zaragoza, Academia General Militar, Carretera de Huesca, s/n, Zaragoza 50090, Spain

[3]Department of Materials Science and Technology - EINA, Instituto de Investigación en Ingeniería de Aragón, I3A, Universidad de Zaragoza, 50018, Spain

[4]Department of Physical Chemistry, Faculty of Sciences, University of Malaga, 29071, Spain

Correspondence to: A. Ansón-Casaos (E-mail: alanson@icb.csic.es)

**ABSTRACT:** Poly(methyl methacrylate) (PMMA) composites containing raw or purified single-walled carbon nanotubes (SWCNTs) are prepared by *in situ* polymerization and solution processing. The SWCNTs are purified by centrifugation in a Pluronic surfactant, which consists of polyethyleneoxide and polypropyleneoxide blocks. Both the effects of SWCNT purity and non-covalent functionalization with Pluronic are evaluated. Electrical conductivity of PMMA increases by 7 orders of magnitude upon the integration of raw or purified SWCNTs. The best electrical properties are measured for composites made of purified SWCNTs and prepared by *in situ* polymerization. Strains at fracture of the SWCNT/PMMA composites are nearly identical to those of the neat matrix. A certain decrease in the work to fracture is measured, particularly for composites containing purified SWCNTs (−31.6%). Fractography and Raman maps indicate that SWCNT dispersion in the PMMA matrix improves upon the direct addition of Pluronic, while dispersion becomes more difficult in the case of purified SWCNTs. © 2014 Wiley Periodicals, Inc. J. Appl. Polym. Sci. **2015**, *132*, 41547.

**KEYWORDS:** composites; graphene and fullerenes; nanotubes; surfactants

Received 28 May 2014; accepted 18 September 2014

**DOI: 10.1002/app.41547**

## INTRODUCTION

Carbon nanotubes (CNTs) have been extensively studied as fillers in polymeric matrices, and substantial improvements in the electrical, mechanical, and thermal properties of the polymers have been reported.[1] Main difficulties for CNT integration in polymers are the strong tendency of CNTs to aggregate, the control of CNT orientation and the weak adhesion between CNTs and the matrices. Ideally, single-walled carbon nanotubes (SWCNTs) should be preferred as polymer fillers, as they have higher aspect ratios than multi-walled carbon nanotubes (MWCNTs). Experimentally, polymer reinforcement and conductivity improvements are usually greater with MWCNTs than with SWCNTs.[2] SWCNT characteristics, including bundling, depend on the synthesis method. Currently, a few companies produce relatively large amounts of SWCNTs with high structural qualities by the arc-discharge method. Typically, pristine arc-discharge SWCNTs contains substantial amounts of graphite, amorphous carbon, and metal catalysts.

Composites of CNTs and poly(methyl methacrylate) (PMMA) are attractive since PMMA has many applications in biomedical technology or as a glass substitute in architectural design and optics. Some improvements in the mechanical performance of PMMA have been achieved, particularly when composites are processed as fibers.[2] Orientation of MWCNTs along the fiber axis by melt drawing can increase tensile toughness by a factor of 2.7,[3] and the direct integration of pristine SWCNTs in electro-spun or melt-extruded PMMA fibers produces improvements in tensile toughness (3.3×) and impact strength (4.0×), although Young's modulus remains approximately unchanged.[2,4] Another approach to efficiently take advantage of CNT properties is the fabrication of composite thin films. Sheet resistances of 80–140 Ω/sq at transmittances of about 80% have been measured for films made of arc-discharge SWCNTs in a water-borne PMMA binder.[5,6] In spite of all these achievements, difficulties arise whenever it is intended to prepare bulk SWCNT/PMMA composites in a large scale.[7] In this context, promising results

have been achieved with SWCNT/PMMA composites prepared by the coagulation method.[8]

The strongest CNT adhesion to polymer matrices, resulting in the greatest improvements in the composite mechanical properties, is obtained through chemical strategies, mainly the covalent attachment of reactive functional groups.[9] The greatest improvements in MWCNT/PMMA tensile properties have been measured for composite films fabricated by *in situ* polymerization of MMA in the presence of hydroxyl-functionalized MWCNTs.[10] Increases in Young's modulus, breaking strength, ultimate tensile strength, and toughness of 1.9, 4.7, 4,6, and 13.7 times, respectively, were observed after the addition of <0.5 wt % of the PMMA-functionalized MWCNTs.[10] Other outstanding findings have been reported for SWCNTs treated with hydroxylamine hydrochloric acid salt,[11] $SOCl_2$-doped SWCNTs,[12] or PMMA modified with imidazolium-based ionic liquid groups.[13] More recently, it has been demonstrated that the presence of strongly oxidized domains in graphene oxide is positive for its integration in PMMA.[14] However, those chemical modifications may simultaneously lead to the loss of other CNT or polymer properties that are required in multifunctional materials.[15]

Increasing CNT compatibility through non-covalent methods would be preferable since it does not affect the CNT electronic structure and electrical properties. Strategies involving the addition of certain amounts of polymers have been investigated for improving MWCNT dispersion and adhesion to PMMA. For example, amine-terminated poly(ethylene oxide) (PEO) was used as a compatibilizer since PEO is miscible with PMMA and amine groups link to carboxylated MWCNTs.[16] In another study, noncovalent functionalization of MWCNTs was accomplished by wrapping with polythiophene-graft-PMMA, resulting in PMMA composite films with increased Young's modulus and unchanged elongation at break.[17] The adsorption of block copolymers on SWCNTs can also improve their adhesion to the matrix and their dispersion in solvents and in the polymer matrix. Poly[methyl methacrylate-*co*-(fluorescein O-acrylate)] has been investigated as a surfactant for the dispersion of SWCNTs in dimethylformamide and their integration in PMMA. At a 2 wt % loading, tensile modulus and strength increased by 1.6 and 1.3 times, respectively, while elongation at break decreased to the 50% of its original value.[18] A possible drawback of using surfactants or polymers for SWCNT noncovalent functionalization is that the insulating properties of those agents may have an adverse influence on the formation of conductive SWCNT networks.

In this work, the block copolymer Pluronic® F68 was investigated as a noncovalent agent for improving the integration of arc-discharge SWCNTs into bulk PMMA. Pluronic F68, a commercial product registered by BASF, is a block copolymer containing polyethyleneoxide (PEO) and polypropyleneoxide (PPO) blocks with a sequence $PEO_x$-$PPO_y$-$PEO_x$ ($M_w = 8400$ g/mol, 80% PEO). The PEO block is hydrophilic and miscible with PMMA, while the PPO block preferentially adsorbs on the SWCNTs. Therefore, wrapping SWCNTs with Pluronic is expected to improve their stability in water and their miscibility with PMMA. In addition, centrifugation of arc-discharge SWCNT suspensions in Pluronic solutions greatly improves the SWCNT purity.[19,20] Here, we study the effect of both Pluronic wrapping and SWCNT purification in the electrical conductivity and tensile properties of bulk SWCNT/PMMA composites. So far, the influence of SWCNT purity has been only controlled for certain polymer matrices different from PMMA.[21] Other effects, such as SWCNT aggregation and interfacial interactions, are assessed by fractography analysis, differential scanning calorimetry (DSC), and Raman spectroscopy mapping.

## EXPERIMENTAL

### SWCNT Synthesis, Purification, and Characterization

SWCNTs were synthesized by the arc discharge method using a Ni/Y (2/0.5 at %) catalyst. As-grown SWCNTs (AG-SWCNTs) have lengths of >1 $\mu$m and diameters ranging from 1.2 to 1.5 nm. However, nanotubes are rarely individualized, and arrange into bundles which reach diameters up to 25 nm. The AG-SWCNT material contains ~13.2 wt % catalyst particles (10.5 wt % Ni, 2.7 wt % Y), graphitic shells, and amorphous carbon impurities.

AG-SWCNTs were purified by a two-stage process consisting of thermal oxidation and centrifugation in a Pluronic F68 solution. In a typical preparation, 300 mg of the AG-SWCNT powder was spread on a Petri dish and treated in an oven at 350°C for 2 h. Approximately 45 wt % of the starting powder was lost during the thermal treatment due to the partial combustion of carbon materials. In a second stage, 200 mg of the thermally oxidized nanotubes (Ox-SWCNTs) were dispersed in 50 mL of a 1 wt/vol % Pluronic F68 (Sigma P1300) aqueous solution. The dispersion was accomplished by 60 min ultrasound treatment with a DRH-P400S tip (Hielscher, Teltow, Germany, 400 W maximum power, 24 kHz maximum frequency) working at 60% amplitude and 0.5 cycles. The SWCNT dispersion was centrifuged at 13,000 rpm (23,000 × *g*) for 30 min in a Z383 universal high speed centrifuge (Hermle Labortechnik, Wehingen, Germany). The resulting supernatant was decanted and the sediment was discarded. The purified SWCNT (P-SWCNT) dispersion was coagulated with ~300 mL of methanol, and was vacuum filtered through polycarbonate filters (Isopore 3 $\mu$m). Subsequently, the solid was washed with ~400 mL of water. The resulting dry material is hereafter called Plu/P-SWCNT, indicating that a certain amount of Pluronic remains adsorbed on the P-SWCNTs.

Near infrared (NIR) absorption spectroscopy of the P-SWCNT dispersion was performed in a 2 mL quartz cubette using a Bruker VERTEX 70 spectrometer. Absorbance measurements in the visible region were performed in a Shimadzu UV-2401PC spectrometer. All the dispersions were diluted with 1% Pluronic F68 solutions to adjust the absorbance into an appropriate range. Thermogravimetric analysis (TGA) of the Plu/P-SWCNT powder was carried out in a Setsys Evolution balance (Setaram) working at a 5°C/min heating rate in an argon flow. Scanning electron microscopy (SEM) was performed in a Hitachi S-3400N microscope. Transmission electron microscopy (TEM) images were obtained in a JEOL-200FXII microscope at 200 kV. For TEM observations, a small amount of the Plu/P-SWCNTs

**Table I.** Nomenclature, Characterization Techniques, and SWCNT Filler Contents (wt %) for all the Prepared Composite Samples

| Sample[a] | Polymerization | Electrical[b] | Electrical[c] | Tensile[c] | SEC[c] | DSC[c] | FESEM[c] | Raman[c] |
|---|---|---|---|---|---|---|---|---|
| PMMA | – | 0% | 0% | 0% | 0% | 0% | 0% | – |
| Plu/PMMA | *In situ* | 0% | 0% | 0% | 0% | 0% | 0% | – |
| AG-SWCNT/PMMA-E | *Ex situ* | 1.1, 1.6, 2.7, 6.0% | – | – | – | – | – | – |
| Plu/P-SWCNT/PMMA-E | *Ex situ* | 1.1, 2.3, 3.8% | – | – | – | – | – | – |
| AG-SWCNT/PMMA-I | *In situ* | 2.4, 3.8, 6.9% | 1.0% | 1.0% | 1.0% | 1.0% | 1.0% | 1.0% |
| Plu/Ox-SWCNT/PMMA-I | *In situ* | – | 1.0% | 1.0% | 1.0% | 1.0% | 1.0% | 1.0% |
| Plu/P-SWCNT/PMMA-I | *In situ* | 0.9, 2.2, 6.2% | 1.0% | 1.0% | 1.0% | 1.0% | 1.0% | 1.0% |

[a] All the Plu/samples contain 0.4 wt % of Pluronic block copolymer.
[b] Electrical properties for specimens sintered by heating at 150°C.
[c] Data for specimens sintered by melt pressing at 200°C and 20 kN.

was ultrasonically dispersed in ethanol and dropped onto a Lacey grid.

### Preparation of Composites for Conductivity Measurements

Composite SWCNT/PMMA samples with various AG-SWCNT and Plu/P-SWCNT contents were prepared by both *in situ* polymerization and solvent mixing. Nomenclature and composition of all the samples is detailed in Table I, where filler amounts indicate the SWCNT material excluding Pluronic. Pluronic content in the Plu/P-SWCNT material was of 29 wt % according to the TGA (see the Results section).

For *in situ* polymerization of PMMA, different amounts of SWCNTs were mixed with 2 mL of methyl methacrylate monomer (MMA, Aldrich M55909) and 10 mL of chloroform. The mixture was subsequently treated with an ultrasound tip (Hielscher DRH-P400S, 60% amplitude, 0.5 cycles) for 5 min, in an ultrasound bath for 1 h, again with the tip for 5 min and finally in the bath for 30 min. Then, 75 mg of benzoyl peroxide initiator (75%, Aldrich 517909) was added to the mixture and it was refluxed at 80°C for 2 h under stirring. The PMMA material was obtained by coagulation in 350 mL of methanol, followed by settling, decantation, and drying. The polymerization mass yield was used to recalculate the SWCNT content in the composite, considering that SWCNT mass is conserved during the whole process. Pure PMMA was polymerized from the monomer following an analogous procedure. A coagulation/decantation protocol was chosen for the present work since it has been observed that SWCNT dispersion in PMMA is better than in direct solvent casting fabrication.[8]

**Table II.** Composition of the Composites for Tensile Tests: Filler Content ($X$) and Polymerization Yield ($Y$)

| Sample | Filler type | $X$ (mg) | $Y$ (g) |
|---|---|---|---|
| AG-SWCNT/PMMA-I | AG-SWCNT | 333 | 21.8 |
| Plu/PMMA | Pluronic F68 | 136 | 25.6 |
| Plu/Ox-SWCNT/PMMA-I | Pluronic F68 | 136 | 17.7 |
| | Ox-SWCNT | 331 | |
| Plu/P-SWCNT/PMMA-I | Plu/P-SWCNT | 469 | 13.7 |

Pure PMMA was added to reach a total disk mass of 33.14 g in each case. Four test specimens were cut from each disk.

For composite synthesis by direct solvent mixing, previously polymerized PMMA and SWCNTs were dispersed in 10 mL of chloroform and sonicated as described for the *in situ* process. The mixture was refluxed at 80°C for 2 h under stirring and coagulated in 350 mL of methanol. The SWCNT content was recalculated after weighing the dried composite. Approximately 140 mg of the coagulated composite materials were sintered at 150°C for 10 min in a cylindrical stainless steel mould ($d = 13$ mm, $t = 1$ mm) between two Teflon plates. Nomenclature for the sintered samples (Table I) includes the "-I" or "-E" at the end to indicate that the composites are prepared by *in situ* polymerization or solvent mixing (*ex situ*), respectively.

### Preparation of Composites for Tensile Tests

Tensile tests were performed on SWCNT/PMMA composites containing exactly 1 wt % of the SWCNT material. The composites were prepared by *in situ* polymerization, and pure PMMA was added and mechanically mixed to adjust the SWCNT content. Besides the AG-SWCNT/PMMA-I and Plu/P-SWCNT/PMMA-I materials, three reference samples were also prepared: pure PMMA, a composite with Pluronic F68 (Plu/PMMA), and a composite with noncentrifuged Pluronic-wrapped Ox-SWCNTs (Plu/Ox-SWCNT/PMMA-I). The nomenclature and composition of all the materials is summarized in Tables I and II. It could be argued that the specimens for tensile tests were prepared by a combination of *in situ* polymerization and mechanical mixing rather than by a pure *in situ* method. However, we keep our nomenclature for *in situ* composites, as all the SWCNTs had the chance to react with radicals generated during MMA polymerization.

In a typical polymerization experiment, 500 mg of benzoyl peroxide were dissolved in 90 mL of chloroform. The SWCNT filler was dispersed in the solution by treatment in an ultrasound bath for 10 min. Then, 50 mL of MMA were added, and the mixture was refluxed at 70°C for 5 h. The product was coagulated in methanol, separated by decantation and dried in an oven. Average yields in pure PMMA polymerizations were around 50% of the initial MMA mass, and polymerization yields obtained in the preparation of the different composites

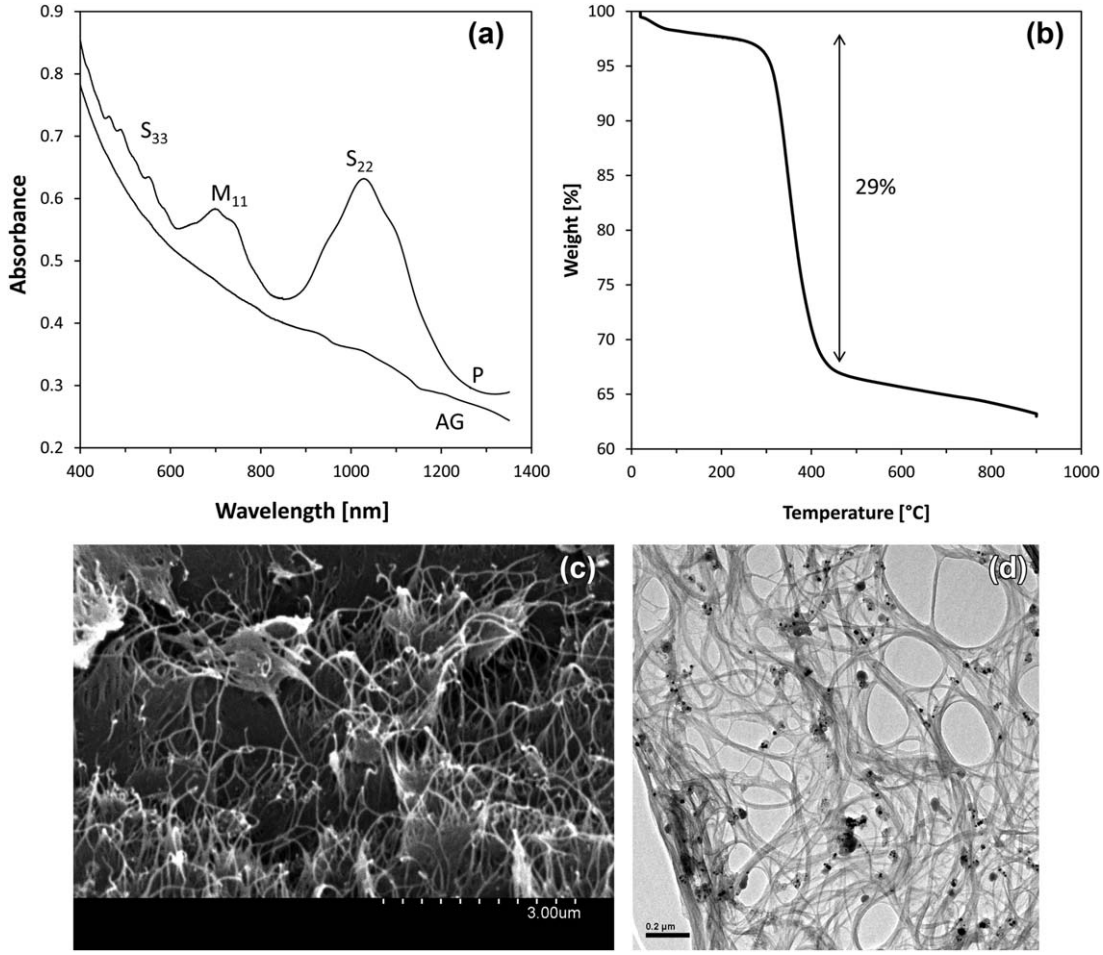


**Figure 1.** Characterization of Pluronic-wrapped SWCNTs: (a) Visible-NIR absorption spectrum of the centrifuged SWCNT dispersion (P-SWCNT) compared with the as-grown SWCNT dispersion (AG-SWCNT), and (b) TGA, (c) SEM image, and (d) TEM image of the Pluronic-wrapped SWCNTs after filtration (Plu/P-SWCNT material).

were of 30–40%. Pure PMMA was added to the solid mixture until completing 33.14 g of total mass. In the case of the Plu/Ox-SWCNT/PMMA-I reference sample, the Plu/Ox-SWCNT filler was prepared by tip sonication of 331 mg of Ox-SWCNTs in an aqueous solution containing 136 mg of Pluronic F68, followed by the slow evaporation of the water solvent.

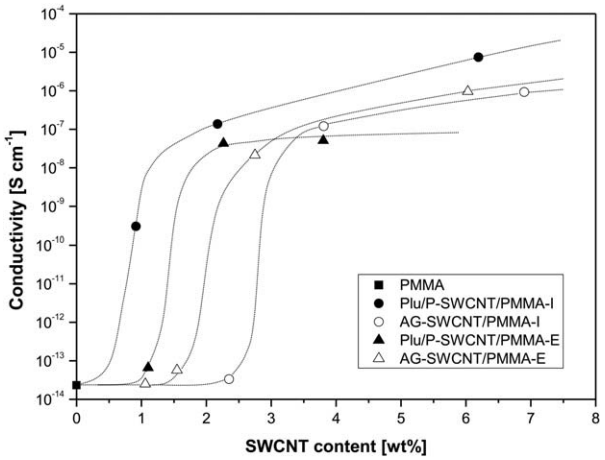


**Figure 2.** Electrical conductivity of various SWCNT/PMMA composites prepared by either *in situ* polymerization or solvent mixing (*ex situ*) methods.

Mixtures containing SWCNTs, *in situ* polymerized PMMA and pure PMMA (33.14 g of total mass) were grinded in a laboratory blade grinder. The resulting powder samples were inserted in a stainless steel mould and sintered at 200°C under 20 kN for 1 h in a Specac laboratory press provided with hot plates (Specac, Slough, UK). Composites were obtained in the shape of flat disks ($d = 90$ mm, $t = 4$ mm) and then cut into standard dog-bone test samples, according to ASTM D 638 M type III. Here, hot-pressing was used instead of thermal sintering with the aim of improving mechanical properties. In addition, the alternative use of hot-pressing allows a comparison between the electrical conductivities obtained by different sintering protocols.

### Characterization of SWCNT/PMMA Composites

Direct current (DC) electrical conductivity was measured with a Keithley 4200-SCS source measurement unit. The samples were placed in a sandwich-like arrangement between two copper sheets of $\sim 1 \times 1$ cm$^2$. Measurements were carried out in a two-probe configuration, with each copper sheet working as an

**Table III.** Tensile Properties and Electrical Conductivity ($\sigma$) for PMMA and Various SWCNT/PMMA Samples Containing 1 wt % of SWCNTs

| Sample | $E_s$ (GPa) | $\sigma_f$ (MPa) | $\varepsilon_f$ (%) | $W_f$ (MJ m$^{-3}$) | $\sigma$ (S cm$^{-1}$) |
|---|---|---|---|---|---|
| PMMA | 0.80 ± 0.02 | 45.7 ± 3.7 | 6.8 ± 0.5 | 1.9 ± 0.5 | 2.4 $10^{-13}$ |
| AG-SWCNT/PMMA-I | 0.75 ± 0.03 | 39.1 ± 3.0 | 6.4 ± 0.5 | 1.5 ± 0.2 | 9.5 $10^{-8}$ |
| Plu/PMMA | 0.84 ± 0.01 | 49.7 ± 2.4 | 7.6 ± 0.7 | 2.1 ± 0.3 | 2.2 $10^{-13}$ |
| Plu/Ox-SWCNT/PMMA-I | 0.81 ± 0.02 | 43.2 ± 1.2 | 6.7 ± 0.1 | 1.7 ± 0.1 | 1.5 $10^{-8}$ |
| Plu/P-SWCNT/PMMA-I | 0.69 ± 0.02 | 35.0 ± 1.3 | 6.7 ± 0.3 | 1.3 ± 0.1 | 1.3 $10^{-7}$ |

electrode. In a typical measurement, the intensity was registered during 10–15 s at a constant voltage of 20 V, and the final value was taken after a plateau was reached.

Tensile specimens were tested to breakage in an Instron Model 5565 test frame. Experiments were performed at room temperature (23 ± 2°C) and 10 mm/min strain rate. At least three tensile specimens were tested per cohort. Engineering stress-strain curves were registered and relevant mechanical parameters (secant modulus, stress and strain at fracture, and work to fracture) were calculated from them.

Molecular weight determinations were performed by size exclusion chromatography (SEC). The analyses were carried out on a chromatographic system (Waters Division Millipore) equipped with a Waters model 410 refractive-index detector. Dimethyl formamide (Aldrich) containing 0.1% of LiBr, was used as the eluent at a flow rate of 1 mL/min at 50°C. Styragel packed columns (HR2, HR3, and HR4, Waters Division Millipore) were used. PMMA standards (Polymer Laboratories, Laboratories) between 2.4 × $10^6$ and 9.7 × $10^2$ g mol$^{-1}$ were used to calibrate the columns.

DSC experiments were performed in a Mettler TA4000 calorimeter operating under a nitrogen flow of 60 cm$^3$/min. Samples ranging between 9 and 18 mg were placed in aluminum crucibles and were heated to 200°C at 10°C/min to erase their thermal history. Then, they were cooled down to −50°C and heated again up to 200°C at 10°C/min.

Fractography analysis was conducted on fractured surfaces of the tensile specimens. This was performed after Au-coating of the samples using a sputtering device (Balzers SCD-4). Samples from specimens in each group were observed with a Field Effect Scanning Electron Microscope (FESEM) model Gemini (Carl Zeiss, Switzerland) in the secondary electron mode at 5 keV, with working distance about 13.5 mm for the higher magnification and probe current of 300 pA.

Micro-Raman maps were measured in a Horiba Jobin Ybon spectrometer (model HR 800 UV) working with a laser at 785 nm, a diffraction network of 1800 grooves/mm, and a 50× objective in the optical microscope. The acquisition range was 140–190 cm$^{-1}$, and the exhibition time was fixed at 2 s in one accumulation period. Raman maps were measured in two ranges, hereafter called the short range (50 × 50 $\mu$m$^2$, pixel size of 1 $\mu$m) and the long range (500 × 500 $\mu$m$^2$, pixel size of 10 $\mu$m).

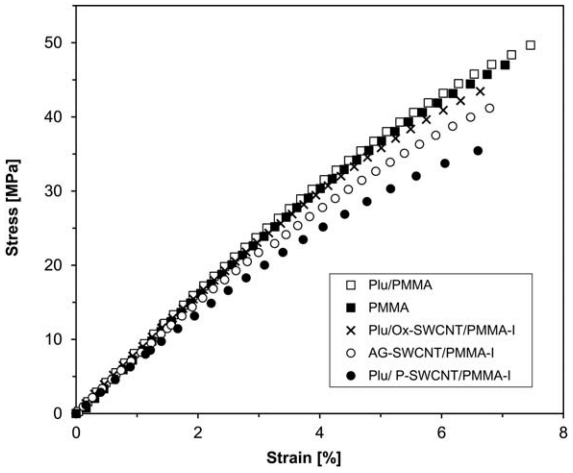


**Figure 3.** Plots showing engineering stress versus strain for PMMA, Plu/PMMA, and various SWCNT/PMMA-I composites at 1.0 wt % SWCNT loading.

## RESULTS

### Characterization of the Purified SWCNTs

Figure 1 summarizes the characterization of the Plu/P-SWCNT sample. The visible/NIR spectrum of the P-SWCNT dispersion [Figure 1(a)] presents the $M_{11}$, $S_{22}$, and $S_{33}$ bands associated to electronic transitions of metallic (M) and semiconducting (S) SWCNTs. The band shapes and positions are associated to the distribution of SWCNT diameters and chiralities. For the arc-discharge SWCNTs used in this study, a purity ratio can be defined as the background-subtracted area of the $S_{22}$ band transition at 7750–11,750 cm$^{-1}$ divided by the total band area. The purity ratio, which is a relative measurement of the content in SWCNTs and carbonaceous impurities, was 0.248 for the P-SWCNT dispersion, in contrast with 0.040 for AG-SWCNTs. Therefore, the purification treatment eliminated most of the graphitic and amorphous carbon impurities, increasing the relative intensity of the characteristic SWCNT spectral bands.

TGA in argon of the Plu/P-SWCNT solid [Figure 1(b)] presents one main weight loss at 346°C associated to the total gasification of the residual Pluronic F68 content. Therefore, 29 wt % of the Plu/P-SWCNT material was really Pluronic F68 wrapping the nanotubes. Minor weight losses below 200°C are due to moisture and labile functional groups, while weight losses above 500°C may correspond to the most stable oxygen functional groups on the carbon surfaces. Figure 1(c,d) show SEM and

**Table IV.** Molecular Masses ($M_n$ and $M_w$) and Dispersity ($D_M$) from SEC, and Glass Transition Temperatures ($T_g$) from DSC, for PMMA and Various SWCNT/PMMA Samples Containing 1 wt % of SWCNTs

| Sample | $M_n$ (Da) | $M_w$ (Da) | $D_M$ | $T_g$ (°C)[a] | $T_g$ (°C)[b] |
|---|---|---|---|---|---|
| PMMA | 77,600 | 151,700 | 1.70 | 105 | 109 |
| AG-SWCNT/PMMA-I | 63,200 | 119,000 | 1.88 | 110 | 115 |
| Plu/PMMA | 87,400 | 139,400 | 1.60 | 110 | 115 |
| Plu/Ox-SWCNT/PMMA-I | 66,490 | 106,570 | 1.60 | 110 | 113 |
| Plu/P-SWCNT/PMMA-I | 60,025 | 115,600 | 1.93 | 110 | 117 |

[a] Cooling scan.
[b] Heating scan.

TEM images of Plu/P-SWCNTs. It is evident that SWCNT bundles are covered by a layer of Pluronic F68 block copolymer, in agreement with the TGA. In addition, the TEM image confirms the elimination of amorphous and graphitic carbon impurities and reveals the persistence of some catalyst metal particles.

### Electrical Conductivity

Figure 2 shows DC conductivity data for pure PMMA and various SWCNT/PMMA composites sintered by heating at 150°C. The results are compared in terms of the composite preparation method (either *in situ* or *ex situ* polymerization) and the filler type (either AG-SWCNTs or Plu/P-SWCNTs). Two interesting parameters can be extracted from the graph: the electrical conductivity improvement due to the filler and an approximate value of the percolation threshold.[1] The highest conductivity ($7.4 \times 10^{-6}$ S cm$^{-1}$ at a 6.2 wt % loading) was found for composites prepared by *in situ* polymerization and containing Plu/P-SWCNTs. However, high conductivities were also measured for composites containing AG-SWCNTs ($9.2 \times 10^{-7}$ S cm$^{-1}$ at 6.9 wt % of filler) or prepared by the *ex situ* solvent mixing method ($9.6 \times 10^{-7}$ S cm$^{-1}$ at 6.0 wt % of filler). Such values are ~8 orders of magnitude higher than the conductivity of neat PMMA ($2.3 \times 10^{-14}$ S cm$^{-1}$), in good agreement with previous results.[8,22,23] This effect was confirmed by conductivity measurements on the specimens prepared for tensile measurements, which were sintered under additional temperature and pressure conditions of 200°C and 20 kN (Table III). It has to be mentioned that ultimate conductivities of the composites are relatively low compared with some other literature reports.[1]

In some early works, *in situ* polymerization of MMA on SWCNTs was proposed as a method to improve SWCNT dispersion and to create chemical bonds between SWCNTs and the PMMA matrix.[24] Those chemical bonds on the SWCNTs should cause a decrease in their electrical conductivity, as they create defects in the nanotube wall structure, hindering electron conduction.[15] More recently, it has been suggested that chemical bonds between SWCNTs and PMMA chains form during *in situ* polymerization only if the SWCNTs are previously functionalized with carboxyl groups, but do not form on raw SWCNTs.[7] Accordingly, *in situ* polymerization of PMMA on AG-SWCNTs is not expected to damage the SWCNT electrical properties. Our results confirm that similar conductivities can be reached for AG-SWCNT/PMMA composites prepared by *in situ* and *ex situ* methods, indicating that both contain AG-SWCNTs with no covalent functionalization.

Approximate values of the percolation threshold can be graphically estimated from Figure 2. It can be observed that the percolation threshold of the *in situ* polymerized Plu/P-SWCNT/

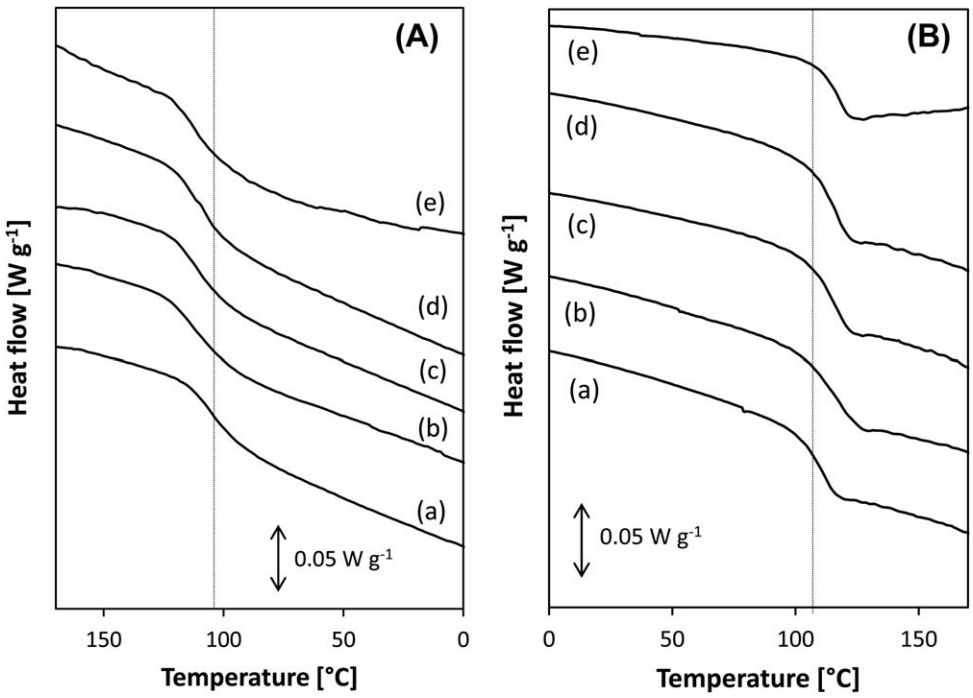


**Figure 4.** DSC cooling (A) and heating (B) profiles for the samples: (a) PMMA, (b) AG-SWCNT/PMMA-I, (c) Plu/PMMA, (d) Plu/Ox-SWCNT/PMMA-I, and (e) Plu/P-SWCNT/PMMA-I.

PMMA-I composite (<1 wt %) was lower than for the Plu/P-SWCNT/PMMA-E composite (~1.2 wt %), prepared by solution mixing. This behavior is in agreement with previously reported results for MWCNT/PMMA composites.[25] Regarding the effect of SWCNT purity, the composites containing the Plu/P-SWCNT material demonstrated lower percolation thresholds than the composites with AG-SWCNTs. Moreover, the purity effect seems to be more important than the change in the preparation method. Overall, the electrical properties of Plu/P-SWCNT/PMMA-I composites were somewhat better than the others. From conductivity measurements on the samples prepared for tensile tests (Table III), it can be deduced that percolation thresholds decrease when the composites are sintered under high temperature and pressure conditions.

### Tensile Properties

Figure 3 shows engineering stress vs strain for the composites considered in this work. The mechanical parameters calculated from these curves are presented in Table III. It is noteworthy that the sole incorporation of Pluronic® F68 to the PMMA improves the secant modulus ($E_s$) value, the stress at fracture ($\sigma_f$), the strain at fracture ($\varepsilon_f$), and the work to fracture ($W_f$). Such behavior reflects an excellent chemical interaction between the copolymer and the matrix, improving the metrics of the bare PMMA.

The proper SWCNT/PMMA composites are characterized by similar strain at fracture values, very close to the non-filled resin one. In addition, we obtained noticeable variations in $E_s$, $\sigma_f$, and $W_f$ for each composite formulation. More specifically, the addition of AG-SWCNTs caused a decrease in the $E_s$ modulus from 0.80 to 0.75 GPa and a decrease in the $W_f$ from 1.9 to 1.5 MJ $m^{-3}$. This variation can be compensated by the direct addition of Pluronic to nonpurified SWCNTs, leading to an $E_s$ modulus of $0.81 \pm 0.02$ GPa for the Plu/Ox-SWCNT/PMMA-I material. However, in the case of Plu/P-SWCNT/PMMA-I the diminution gets its maximum, and the presence of Pluronic cannot compensate it. The $E_s$ value decreased a 13%, until $0.69 \pm 0.02$ GPa, and the $W_f$ decreased by nearly 32%. In other words, the Plu/P-SWCNT/PMMA-I gets the maximum elongation prior to fracture being subjected to a lower external stress. This flexibilization can improve the material behavior in applications where mechanical compatibility is important, as spine devices.[26]

The tensile measurements on the SWCNT/PMMA composites showed that mechanical properties decrease upon the addition of 1 wt % SWCNTs. According to the literature, it is not expected that substantial improvements could be achieved for higher SWCNT loadings.[10,12,27] On the contrary, improvements could be expected at lower SWCNT loadings, which would possibly lead to the simultaneous loss of the electrical conductivity.

## DISCUSSION

In this section, we try to interpret the electrical and tensile measurements in terms of dispersion and interfacial interaction of the SWCNTs in the PMMA matrix. Our discussion is based on four characterization techniques: SEC, DSC, FESEM fractography and Raman spectroscopy mapping.

SEC analysis allows the calculation of the polymer molar mass ($M_n$ = number average and $M_w$ = mass average) and dispersity ($D_M = M_w/M_n$). These parameters are listed in Table IV for the 1 wt % SWCNT/PMMA composites and pure PMMA after being hot-pressed at 20 kN. In addition, it has to be mentioned that the parameters for nonsintered PMMA ($M_n$ = 90,700 Da; $M_w$ = 147,800 Da; $D_M$ = 1.63) are nearly identical to those for the specimen after hot pressing. Thus, neither further polymerization nor polymer degradation took place during hot-pressing. The presence of SWCNTs during the polymerization process causes a moderate decrease in both $M_n$ and $M_w$, although it does not have a clear effect in $D_M$. The decrease in the molecular weight has been previously associated to the SWCNT capacity to act as a radical scavenger.[28] Since PMMA polymerization follows a radical chain mechanism, SWCNTs accelerate the reaction termination.

In PMMA, which is an amorphous material, the strength of the interfacial interaction between the SWCNT fillers and the matrix can be qualitatively assessed by DSC. Figure 4 shows DSC cooling and heating profiles for all the composites that were mechanically tested in this work. The calculated glass transition temperatures ($T_g$) are listed in Table IV. All the $T_g$ values for SWCNT/PMMA composites are 5–8°C higher than that of neat PMMA. This increment is similar to previously published data for composites prepared by *in situ* polymerization of MMA on PMMA-grafted SWCNTs.[29] A nearly identical change in $T_g$ is measured after the addition of Pluronic without SWCNTs to PMMA. This observation could be explained by some restrictions in the PMMA chain mobility induced after the radical polymerization of MMA in the presence of Pluronic. The mobility restrictions due to SWCNTs, Pluronic, or Pluronic-wrapped SWCNTs lead to nearly identical changes in the $T_g$, which could indicate that the effect of Pluronic prevails when SWCNTs are totally covered by the copolymer. On the contrary, greater changes in $T_g$ values of SWCNT/PMMA composites have been reported in the literature for composites containing aminated SWCNTs (+17°C).[30,31] Therefore, the nanotube/matrix interaction in our composites, which contain pristine or Pluronic-wrapped SWCNTs, does not correspond to highly covalently modified nanotubes. This fact confirms that *in situ* radical polymerization of MMA does not lead to a massive covalent anchoring of PMMA chains on the nanotube surfaces, in agreement with Fraser et al.[7] Moreover, it can be expected that *in situ* polymerization does not strongly modify the SWCNT electronic properties. In fact, *in situ* polymerization does not induce losses in the electrical conductivity, compared with the composites prepared by the *ex situ* solution method (Figure 2).

FESEM fractography provides information about the surface microstructure at the weakest regions in the specimen, where the material firstly fails under stress. Figure 5 presents 2000× micrographs for pure PMMA and Plu/PMMA, and 2000×–20,000× micrographs for the SWCNT/PMMA composites. Images (a) and (c) show the pristine PMMA and the

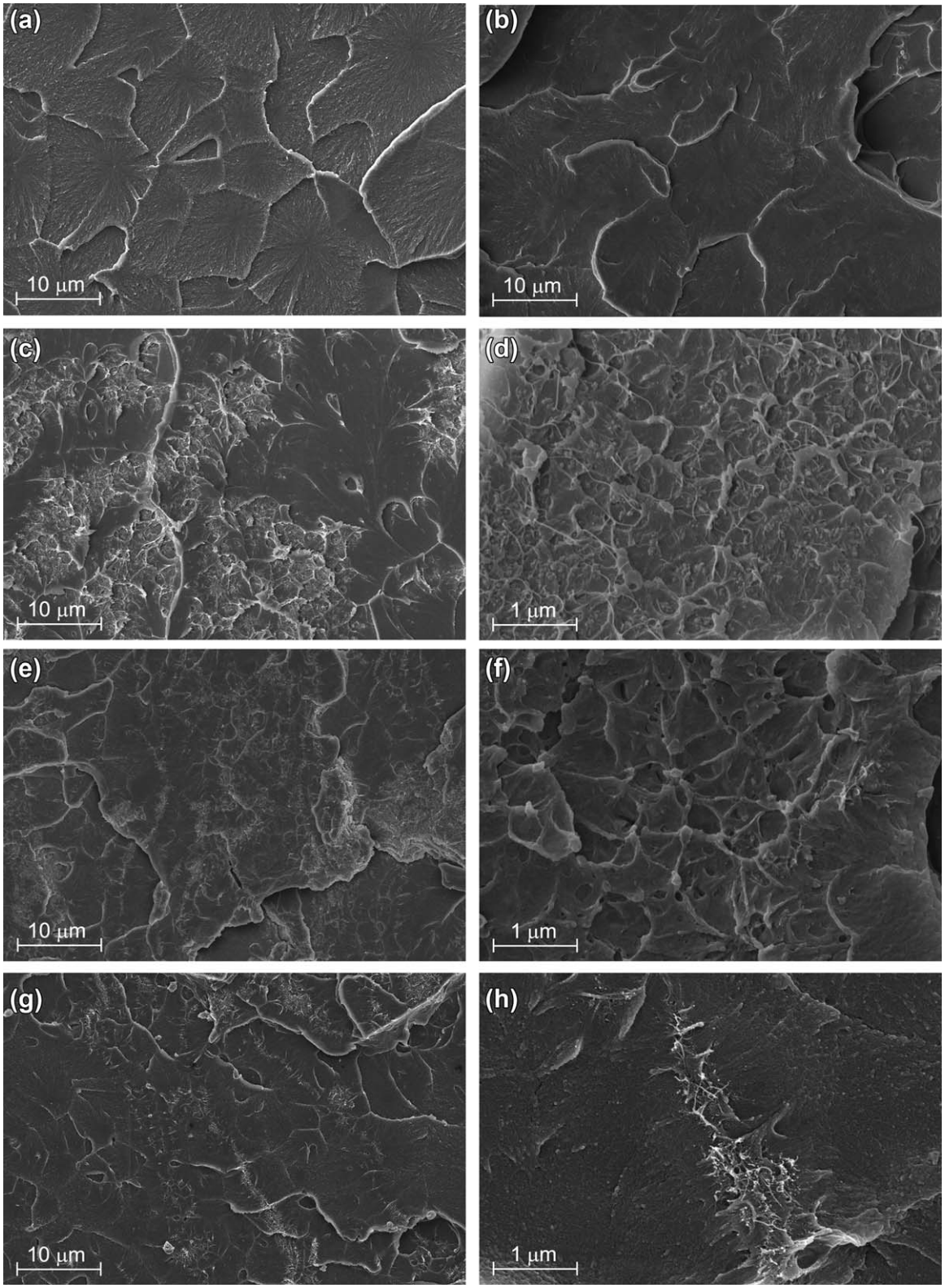


**Figure 5.** FESEM micrographs showing microstructures for: (a) PMMA, (b) Plu/PMMA, (c,d) AG-SWCNT/PMMA-I, (e,f) Plu/Ox-SWCNT/PMMA-I, and (g,h) Plu/P-SWCNT/PMMA-I. Magnification is ×2000 for a, b, c, e, and f, and ×20,000 for d, f, and h. The three SWCNT/PMMA composites are prepared by the *in situ* polymerization method and contain 1 wt % of the SWCNT filler.

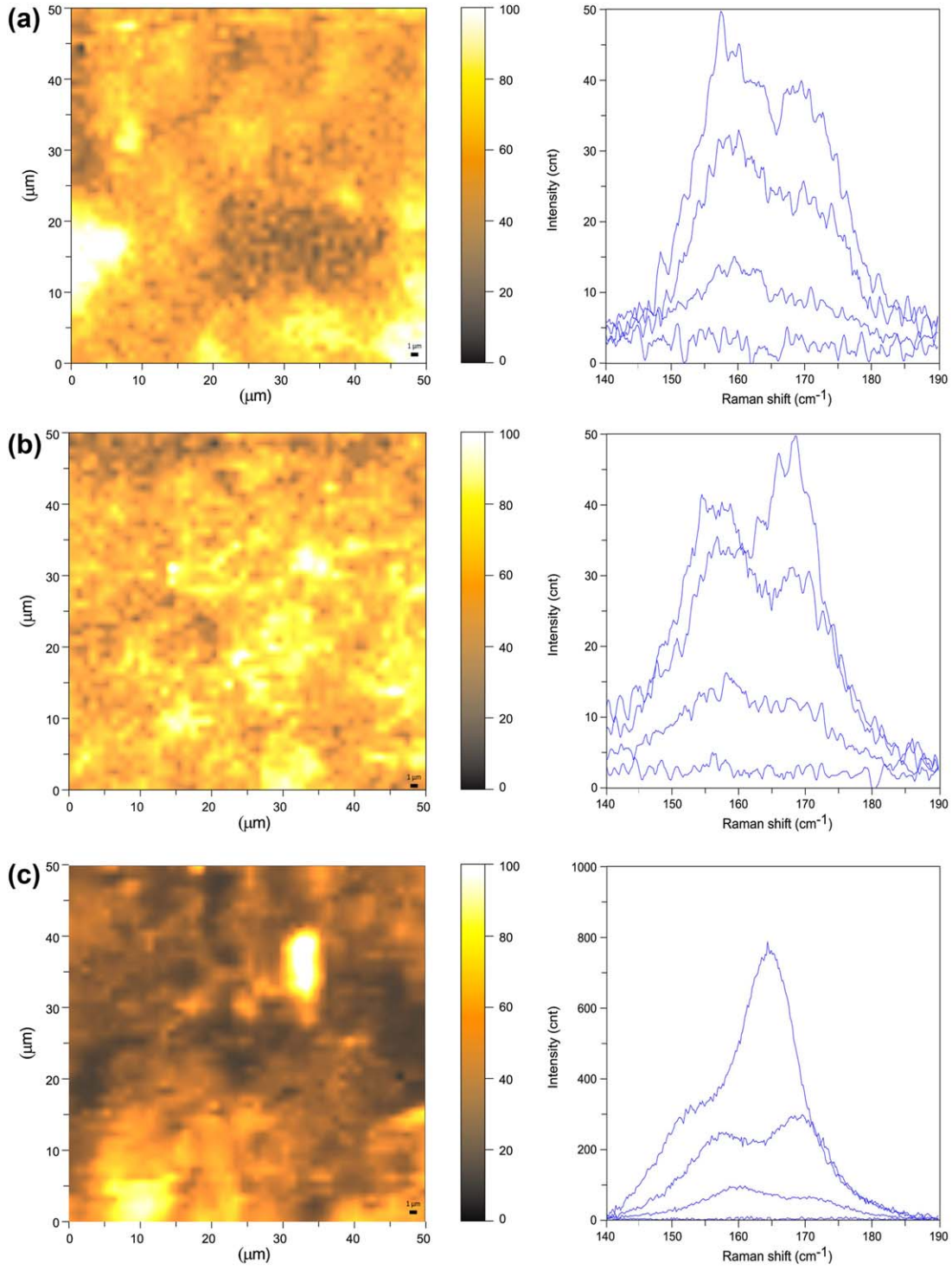


**Figure 6.** Short range Raman maps (50 × 50 $\mu m^2$) for (a) AG-SWCNT/PMMA-I, (b) Plu/Ox-SWCNT/PMMA-I, and (c) Plu/P-SWCNT/PMMA-I. Graphs in the left side show selected spectra including those with the highest and the lowest intensities in each map. [Color figure can be viewed in the online issue, which is available at wileyonlinelibrary.com.]

Plu/PMMA composite respectively. Both images are characterized by a relatively smooth fracture surface, showing the breakage through the grains. AG-SWCNT/PMMA-I and Plu/Ox-SWCNT/PMMA-I micrographs demonstrate the existence of areas much brighter than the mid-gray background that represents the polymer. These areas, identified as SWCNT colonies, are concentrated in wide regions, being unable to transfer mechanical stresses properly and causing a decrease in the ultimate tensile stress. It can be observed that the SWCNT distribution in the material containing Pluronic (Plu/Ox-SWCNT/PMMA-I) [Figure 5(e,f)] is more homogeneous than in the Pluronic-free AG-SWCNT/PMMA-I [Figure

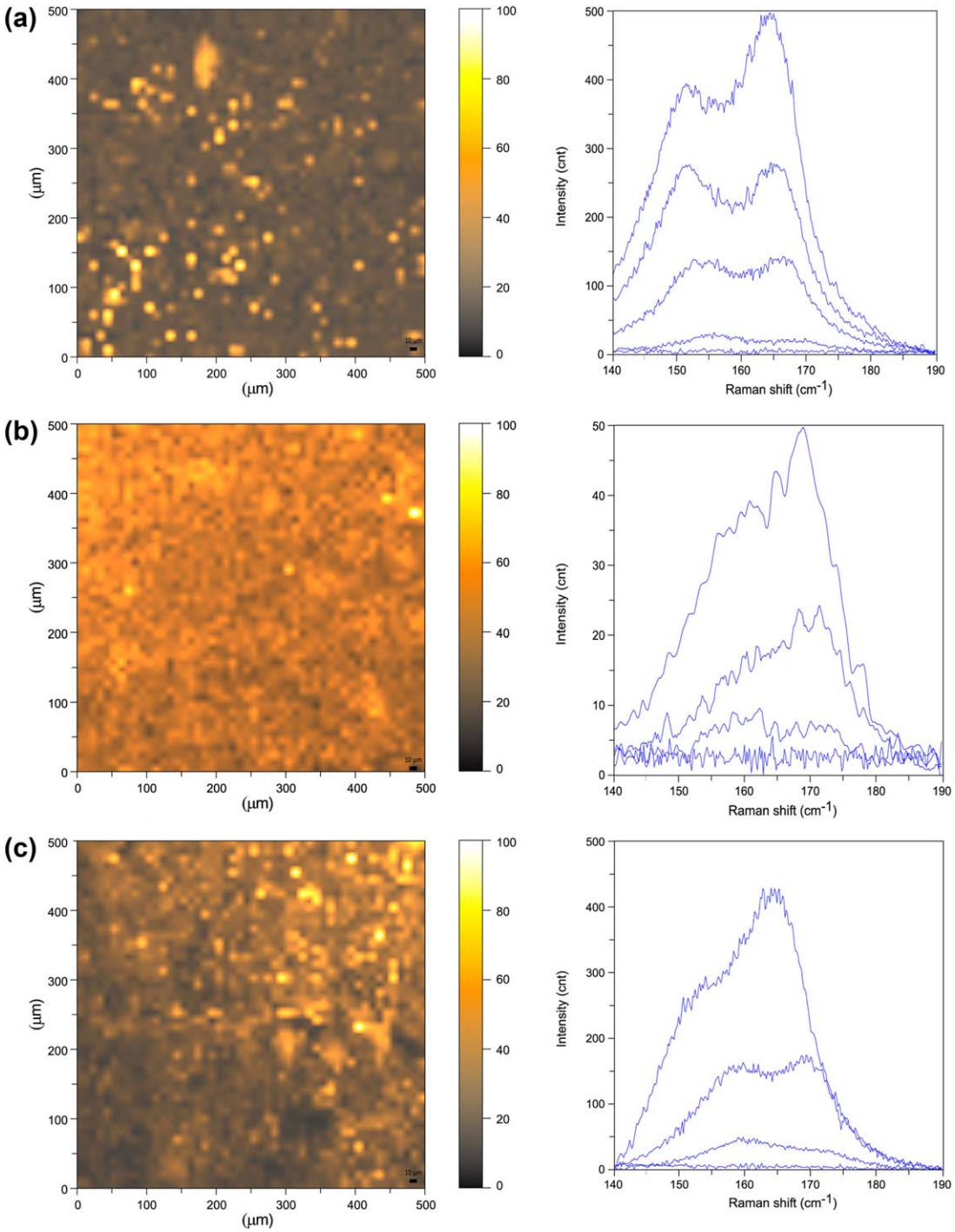


**Figure 7.** Long range Raman maps (500 × 500 $\mu m^2$) for (a) AG-SWCNT/PMMA-I, (b) Plu/Ox-SWCNT/PMMA-I, and (c) Plu/P-SWCNT/PMMA-I. Graphs in the left side show selected spectra including those with the highest and the lowest intensities in each map. [Color figure can be viewed in the online issue, which is available at wileyonlinelibrary.com.]

5(c,d)]. Thus, Pluronic wrapping causes an improvement in the SWCNT dispersion, in agreement with previous results for an epoxy matrix.[32]

The fracture surface of Plu/P-SWCNT/PMMA-I [Figure 5(g,h)] is substantially different from the others. Large SWCNT aggregates with a heterogeneous distribution in the matrix can be observed in the image. Those aggregates cause a poor load transfer between SWCNTs and the matrix, according to the pull-out scheme, and account for the decrease in $E_s$ and in particular $W_f$ for Plu/P-SWCNT/PMMA-I. Whilst Pluronic block copolymer seems to be an efficient compatibility agent, Plu/P-SWCNT dispersion is less efficient than in the case of unpurified SWCNTs. The compatibility effect of Pluronic wrapping could explain the relatively small decrease in the strain at

fracture of Plu/P-SWCNT/PMMA-I compared to pure PMMA.[33] However, it does not prevent the appearance of large chains of aggregated SWCNTs, as it can be seen at the center of Figure 5(e). Those chain-like groups probably contain SWCNTs in an intimate contact, which favor electrical transport, resulting in composites with an improved electrical conductivity. Actually, the conductivity for Plu/P-SWCNT/PMMA-I is higher than for AG-SWCNT/PMMA-I (Table III). Apart from the increase in the number of nanotubes after purification, the positive influence of a certain degree of SWCNT aggregation in the electrical conductivity has been previously suggested in the literature.[34,35]

The FESEM observations regarding SWCNT distribution in the different SWCNT/PMMA composites are confirmed by Raman spectroscopy maps (Figures 6 and 7). Figure 6 shows short-range ($50 \times 50\ \mu m^2$) maps and Figure 7 shows long-range ($500 \times 500\ \mu m^2$) maps, together with various representative spectra in each case. Most of the spectrum profiles show a bimodal distribution, with band maxima centered at 150–160 $cm^{-1}$ and 160–170 $cm^{-1}$, even though the relative intensity of the bands and their maximum positions present some variations through the analyzed regions. For high intensity spectra, the band at 160–170 $cm^{-1}$ is more intense than the band at 150–160 $cm^{-1}$, and presents frequency softening. On the contrary, for low intensity spectra, the band at 150–160 $cm^{-1}$ is the most intense.

As it can be expected, SWCNT/PMMA composite surfaces show more homogeneous SWCNT distributions at the short special range (Figure 6) than at the long range (Figure 7). However, both short and long range maps demonstrate an improvement in the SWCNT homogeneity for the Plu/Ox-SWCNT/PMMA-I composite, compared with the AG-SWCNT/PMMA-I composite. In addition, it can be seen that the Plu/P-SWCNT/PMMA-I surface is more heterogeneous than the Plu/Ox-SWCNT/PMMA-I surface. These observations are in agreement with FESEM images. The presence of Pluronic block copolymer is beneficial for the SWCNT dispersion in PMMA. However, Plu/P-SWCNTs are highly agglomerated and their dispersion is more difficult than in the case of unpurified SWCNTs.

## CONCLUSIONS

Composites containing arc-discharge SWCNTs in a PMMA matrix are prepared by solution processing or *in situ* polymerization of MMA in chloroform, followed by coagulation in methanol. In both cases, the addition of 1–2 wt % SWCNTs increases the PMMA electrical conductivity by at least 7 orders of magnitude. The electrical conductivity and DSC measurements suggest that radical polymerization of MMA in the presence of SWCNTs does not cause a significant covalent modification of the SWCNT surface. According to FESEM images and Raman spectroscopy maps, noncovalent functionalization with Pluronic block copolymer can improve the SWCNT compatibility with the PMMA matrix, favoring their dispersion and thus the composite homogeneity. Pluronic-wrapping can also counteract the decrease in the ultimate tensile stress, secant modulus, and work to fracture produced by the direct addition of AG-SWCNTs. However, SWCNT purification by centrifugation in a Pluronic solution leads to a highly aggregated SWCNT material, which cannot be efficiently dispersed during the composite preparation in chloroform. The Plu/P-SWCNT/PMMA-I composites contain chain-like aggregates that can be observed by FESEM and detected in the Raman maps. The resulting Plu/P-SWCNT/PMMA-I composites demonstrate higher electrical conductivity, lower percolation threshold, similar ultimate tensile strain, and lower work to fracture than AG-SWCNT/PMMA-I composites.

## ACKNOWLEDGMENTS

This work was funded by the Spanish MINECO under the projects TEC2010-15736, MAT2010-16175 (CICYT), CTQ2006-02330, and PRI-PIBAR-2011-1, and the Government of Aragon (DGA) and the European Social Fund (ESF) under Project DGA-ESF-T66 CNN. C. Ruano acknowledges MINECO for her PhD grant BES2007-17250.

## REFERENCES

1. Spitalsky, Z.; Tasis, D.; Papagelis, K.; Galiotis, C. *Prog. Polym. Sci.* **2010**, *35*, 357.
2. Sui, X.; Wagner, H. D. *Nano Lett.* **2009**, *9*, 1423.
3. Gorga, R. E.; Cohen, R. E. *J. Polym. Sci. Part B: Polym. Phys.* **2004**, *42*, 2690.
4. Cooper, C. A.; Ravich, D.; Lips, D.; Mayer, J.; Wagner, H. D. *Compos. Sci. Technol.* **2002**, *62*, 1105.
5. Jung, H.; An, S. Y.; Lim, J. S.; Kim, D. *J. Nanosci. Nanotechnol.* **2011**, *11*, 6345.
6. Jung, H.; Yu, J. S.; Lee, H. P.; Kim, J. M.; Park, J. Y.; Kim, D. *Carbon* **2013**, *52*, 259.
7. Fraser, R. A.; Stoeffler, K.; Ashrafi, B.; Zhang, Y.; Simard, B. *ACS Appl. Mater. Interfaces* **2012**, *4*, 1990.
8. Du, F.; Fischer, J. E.; Winey, K. I. *J. Polym. Sci. Part B: Polym. Phys.* **2003**, *41*, 3333.
9. González-Domínguez, J. M.; Martínez-Rubi, Y.; Diez-Pascual, A. M.; Ansón-Casaos, A.; Gómez-Fatou, M.; Simard, B.; Martínez, M. T. *Nanotechnology* **2012**, *23*, 285702.
10. Blond, D.; Barron, V.; Ruether, M.; Ryan, K. P.; Nicolosi, V.; Blau, W. J.; Coleman, J. N. *Adv. Funct. Mater.* **2006**, *16*, 1608.
11. Sabba, Y.; Thomas, E. L. *Macromolecules* **2004**, *37*, 4815.
12. Skakalova, V.; Dettlaff-Weglikowska, U.; Roth, S. *Synth. Met.* **2005**, *152*, 349.
13. Fukushima, T.; Kosaka, A.; Yamamoto, Y.; Aimiya, T.; Notazawa, S.; Takigawa, T.; Inabe, T.; Aida, T. *Small* **2006**, *2*, 554.
14. Vallés, C.; Kinloch, I. A.; Young, R. J.; Wilson, N. R.; Burke, J. P. *Compos. Sci. Technol.* **2013**, *88*, 158.
15. Gonzalez-Dominguez, J. M.; Diez-Pascual, A. M.; Anson-Casaos, A.; Gomez-Fatou, M. A.; Martinez, M. T. *J. Mater. Chem.* **2011**, *21*, 14948.
16. Wang, M.; Pramoda, K. P.; Goh, S. H. *Carbon* **2006**, *44*, 613.
17. Kim, K. H.; Jo, W. H. *Compos. Sci. Technol.* **2008**, *68*, 2120.
18. Liu, X.; Chan-Park, M. B. *J. Appl. Polym. Sci.* **2009**, *114*, 3414.

19. Anson-Casaos, A.; Gonzalez-Dominguez, J. M.; Martinez, M. T. *Carbon* **2010**, *48*, 2917.
20. Anson-Casaos, A.; Gonzalez-Dominguez, J. M.; Gonzalez, M.; Martinez, M. T. *Langmuir* **2011**, *27*, 7192.
21. Bekyarova, E.; Thostenson, E. T.; Yu, A.; Itkis, M. E.; Fakhrutdinov, D.; Chou, T. W.; Haddon, R. C. *J. Phys. Chem. C* **2007**, *111*, 17865.
22. Chauvet, O.; Benoit, J. M.; Corraze, B. *Carbon* **2004**, *42*, 949.
23. Dai, J.; Wang, Q.; Li, W.; Wei, Z.; Xu, G. *Mater. Lett.* **2007**, *61*, 27.
24. Putz, K. W.; Mitchell, C. A.; Krishnamoorti, R.; Green, P. F. *J. Polym. Sci. Part B: Polym. Phys.* **2004**, *42*, 2286.
25. Yuen, S. M.; Ma, C. C. M.; Chuang, C. Y.; Yu, K. C.; Wu, S. Y.; Yang, C. C.; Wei, M. H. *Compos. Sci. Technol.* **2008**, *68*, 963.
26. Kinzl, M.; Benneker, L. M.; Boger, A.; Zysset, P. K.; Pahr, D. H. *Eur. Spine J.* **2012**, *21*, 920.
27. Ormsby, R.; McNally, T.; O'Hare, P.; Burke, G.; Mitchell, C.; Dunne, N. *Acta Biomater.* **2012**, *8*, 1201.
28. Gonçalves, G.; Cruz, S. M. A.; Ramalho, A.; Gracio, J.; Marques, P. A. A. P. *Nanoscale* **2012**, *4*, 2937.
29. Cui, L.; Tarte, N. H.; Woo, S. I. *J. Appl. Polym. Sci.* **2011**, *119*, 452.
30. Ramanathan, T.; Liu, H.; Brinson, L. C. *J. Polym. Sci. Part B: Polym. Phys.* **2005**, *43*, 2269.
31. Flory, A. L.; Ramanathan, T.; Brinson, L. C. *Macromolecules* **2010**, *43*, 4247.
32. Gonzalez-Dominguez, J. M.; Anson-Casaos, A.; Diez-Pascual, A. M.; Ashrafi, B.; Naffakh, M.; Backman, D.; Stadler, H.; Johnston, A.; Gomez, M.; Martinez, M. T. *ACS Appl. Mater. Interfaces* **2011**, *3*, 1441.
33. Kim, M. T.; Park, H. S.; Hui, D.; Rhee, K. Y. *J. Nanosci. Nanotechnol.* **2011**, *11*, 7369.
34. Bryning, M. B.; Islam, M. F.; Kikkawa, J. M.; Yodh, A. G. *Adv. Mater.* **2005**, *17*, 1186.
35. Kovacs, J. Z.; Velagala, B. S.; Schulte, K.; Bauhofer, W. *Compos. Sci. Technol.* **2007**, *67*, 922.